Temperature dependences of energies and broadening parameters of the band-edge excitons of Re-doped WS_2 and 2H-WS_2 single crystals

2004 J. Phys.: Condens. Matter 16 6995

(http://iopscience.iop.org/0953-8984/16/39/032)

INSTITUTE OF PHYSICS PUBLISHING JOURNAL OF PHYSICS: CONDENSED MATTER

J. Phys.: Condens. Matter **16** (2004) 6995–7005 PII: S0953-8984(04)78690-7

Temperature dependences of energies and broadening parameters of the band-edge excitons of Re-doped WS_2 and 2H-WS_2 single crystals

P C Yen[1], H P Hsu[1], Y T Liu[1], Y S Huang[1,3] and K K Tiong[2]

[1] Department of Electronic Engineering, National Taiwan University of Science and Technology, Taipei 106, Taiwan
[2] Department of Electrical Engineering, National Taiwan Ocean University, Keelung 202, Taiwan

Received 30 March 2004, in final form 30 July 2004
Published 17 September 2004
Online at stacks.iop.org/JPhysCM/16/6995
doi:10.1088/0953-8984/16/39/032

Abstract

The temperature dependences of the spectral features in the vicinity of direct band-edge excitonic transitions for rhenium-doped (Re-doped) and undoped WS_2 single crystals are measured over a temperature range of 15–300 K using piezoreflectance (PzR). From a detailed line shape fit of the PzR spectra, the temperature dependences of the energies and broadening parameters of the A and B excitons are determined accurately. The A and B excitonic transition energies show a red shift and a reduction of their splitting due to the presence of a small amount of Re and the broadening parameter of the excitonic transition features increases due to impurity scattering. The broader line width and the nature of the two-dimensional Mott–Wannier excitons of the 3R polytype prevent the detection of higher Rydberg series for the Re-doped samples. The parameters that describe the temperature variations of the energies and broadening functions of the excitonic transitions are evaluated and discussed.

1. Introduction

The layered transition metal dichalcogenides MX_2 (M = Mo, W, Ta, Nb, V, Ti, Zr, Hf; X = Se, S) have been extensively investigated. Some investigations were mainly related to the lubricating properties of MS_2 [1–4], and others to the photovoltaic properties of MX_2 [5–9]. However, the resource abundance and the nontoxicity of sulfur have to be taken into account for applications. WS_2 has been the subject of great interest, because its bandgap is well matched to the solar spectrum [9]. It can act as an efficient photoconductive layer in photovoltaic devices and photoelectrochemical solar cells [10–12]. The main advantage of WS_2 is the prevention of photocorrosion, because the phototransitions involve nonbonding d–d orbitals

[3] Author to whom any correspondence should be addressed.

of W atoms [13]. Topics investigated commonly deal with the strong anisotropy of physical properties [14], the role of the d orbitals of the transition metal atom in the electronic band scheme [15] and the sharp excitonic structures in the visible region [16, 17]. These structures are generally attributed to the existence of the excitonic transitions A and B characterized by fundamental levels still evident at room temperature. The study of the optical properties of solids has given a good deal of information on the electronic properties and band structures.

It has been found that the doping of WS_2 with rhenium (Re) [18] showed quite a marked difference from that of WSe_2 [19] and $MoSe_2$ [20]. Re-doped WSe_2 and $MoSe_2$ retain the two-layer hexagonal crystal structure (2H-structure). The dopant plays the role of donor impurity with enhancement of electrical conductivity and photocurrent gain [21]. A reduction of electrical anisotropy along and perpendicular to the *c*-axis is also observed [20, 22]. For Re-doped WS_2, the rhenium dopant seems to serve more than just as an impurity donor. It is very likely that the Re ions can substitute for the W metal ions and increase the stability of the rhombohedral structure [18, 23]. It was found that introduction of a small quantity of Re ions during crystal growth of WS_2 can stimulate the formation of three-layer rhombohedral WS_2 (3R-WS_2). In addition, the enhancement of electrical conductivity and a red shift of the indirect band edge were also observed when increasing the Re concentration [18]. The transformation of 2H-WS_2 into 3R-WS_2 by doping with Re concurred with the finding that naturally occurring 3R-WS_2 is consistently rich in certain minor elements such as Re, Nb etc [24]. The ability to synthesize 2H- and 3R-WS_2 offered a potentially attractive venue for studying the influence of Re dopant on the electrical and optical properties of the materials.

In this paper we report a detailed study of the temperature dependence of the piezoreflectance (PzR) measurements in the spectral range of the A and B excitonic features for Re-doped and undoped WS_2 single crystals in the range 15–300 K. PzR has been proven to be useful in the characterization of semiconductors [25, 26]. The derivative nature of modulation spectra suppresses uninteresting background effects and greatly enhances the precision in the determination of interband excitonic transition energies. The sharper lineshape as compared to the conventional optical techniques has enabled us to achieve a greater resolution and hence to detect weaker features. The PzR spectra have been fitted with a form of the Aspnes equation of the first-derivative Lorentzian lineshape [25, 27]. From a detailed lineshape fit we are able to determine accurately the energies and broadening parameters of the excitonic transitions. The physical role of Re in influencing the electronic states of WS_2 has been discussed. Temperature variation of the transition energies of A and B excitons has been analysed by the Varshni equation [28] and an expression containing the Bose–Einstein occupation factor for phonons [29, 30]. The parameters that describe the temperature dependence of the broadening function has been studied in terms of a Bose–Einstein equation that contains the electron (exciton)–longitudinal optical (LO) phonon coupling constant.

2. Experiment

Rhenium-doped WS_2 single crystals have been grown via the chemical vapour transport method with Br_2 as a transport agent. The total charge used in each growth experiment was about 10 g. The stoichiometrically determined weight of the doping material Re was added in the hope that it will be transported at a rate similar to that of tungsten. The quartz ampoule containing Br_2 ($\sim$5 mg cm^{-3}) and uniformly mixed elements (W, 99.99% pure; Re, 99.99%; S, 99.999%) was sealed at 10^{-6} Torr. The ampoule was placed in a three-zone furnace and the charge prereacted for 24 h at 850 °C with the growth zone at 1000 °C, preventing the transport of the product. The temperature of the furnace was increased slowly. The slow heating was necessary to avoid any possibility of explosion due to the exothermic reaction between the

elements. The furnace was then equilibrated to give a constant temperature across the reaction tube, and was programmed over 24 h to produce the temperature gradient at which single-crystal growth took place. Optimal results were obtained with a temperature gradient of approximately 1000 °C → 950 °C. Single-crystalline platelets up to 8×8 mm^2 in surface area and 1 mm in thickness were obtained. WS_2 crystallizes with 2H or 3R structure [14], while ReS_2 crystallizes in a distorted C6 structure [14, 31], so that only a small solubility range is to be expected. It was found that a 5% Re nominal doping of WS_2 prevented the growth of single crystals [18].

Auger electron spectroscopy (AES) was utilized to examine the contents of the Re composition. AES indicates the presence of a small quantity of Re (∼0.1–0.2%) and the concentration of Re in the sample crystals tends to vary from point to point. The nominal concentration of Re is much larger than that determined by AES. The W and Re metals are most likely chemically transported at different rates and most of the Re must remain in the untransported residual charge.

The PzR measurements were achieved by gluing the thin single-crystal specimens on a 0.15 cm thick lead zirconate titanate piezoelectric transducer driven by a 200 V_{rms} sinusoidal wave at 207 Hz. The alternating expansion and contraction of the transducer subjects the sample to an alternating strain with a typical rms $\Delta l/l$ value of $\sim 10^{-5}$. A 150 W tungsten–halogen lamp filtered by a model 270 McPherson 0.35 m monochromator provided the monochromatic light. The reflected light was detected by an EG&G type HUV-2000B silicon photodiode, and the signal was recorded from an NF model 5610B lock-in amplifier. An RMC model 22 closed-cycle cryogenic refrigerator equipped with a model 4075 digital thermometer controller was used for low-temperature measurements. The measurements were made between 15 and 300 K with a temperature stability of 0.5 K or better.

3. Results and discussion

Displayed in figure 1 are the PzR spectra over the range 1.85–2.6 eV at 15 K for the Re-doped and undoped WS_2 single crystals. The spectra are mainly characterized by two prominent A and B excitonic transitions. In the case of undoped WS_2, a higher series of the A exciton and an adjacent antiresonance feature above the A series, denoted as A_2 and A_R, are also detected. In order to determine the positions of the transitions accurately, we performed a theoretical line shape fitting. The functional form used in the fitting procedure corresponds to a first-derivative Lorentzian line shape function of the form [25]

$$\frac{\Delta R}{R} = \mathrm{Re} \sum_{j=1} C_j e^{i\Phi_j} (E - E_j + i\Gamma_j)^{-n} \tag{1}$$

where the subscript j refers to the type of interband transition, C_j and Φ_j are the amplitude and phase of the line shape, E_j and Γ_j are the energy and broadening parameter of the transition and the value of n depends on the origin of the transition. For the first-derivative functional form, $n = 2$ is appropriate for the bounded states, such as excitons or impurity transitions [25]. Least squares fits using equation (1) with $n = 2$ can be achieved and the fits are shown as solid curves in figure 1. The fits yield the parameters C_j, E_j and Γ_j. The obtained values of E_j are indicated as arrows and denoted as A_1, A_2, A_R and B. The notation used here follows closely that of Wilson and Yoffe [14] and Beal *et al* [32]. The fitted values of E_j are displayed in table 1 together with the relevant works of [7, 32–36] for comparison. The values of E_j obtained here show a general agreement with slight deviation from the corresponding low temperature data of [7, 32–34]. We believe the derivative nature of the PzR spectra should offer better accuracy. For undoped WS_2, the exciton A Rydberg series can be described by the three-dimensional

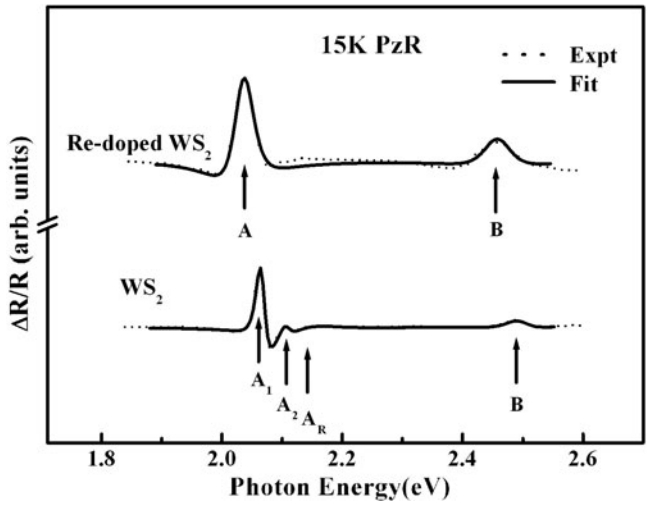

Figure 1. Piezoreflectance spectra for the Re-doped and undoped WS_2 at 15 K. The dashed curves are the experimental curves and the solid curves are least squares fits to equation (1). Arrows under the curves show the energy location for the excitonic features. The antiresonance feature denoted A_R for the undoped WS_2 is also indicated.

Mott–Wannier excitons which follow the relation [32, 34]

$$E_n = E_g - \frac{R}{n^2} \qquad n = 1, 2, 3, \ldots \tag{2}$$

where E_g and R are the exciton-series limit and binding energy respectively. This model predicts that the intensity of the discrete excitonic transition falls off as n^{-3}. The direct bandgap E_g and the binding energy of the exciton A series for pure WS_2 at 15 K are estimated to be 2.119 ± 0.002 eV and 52 ± 2 meV, respectively. The broader line width of the B exciton prevents the detection of higher Rydberg series. For Re-doped WS_2, only the ground state ($n = 1$) of the A exciton is observed. It has been shown that excitons for 3R-WS_2 are more appropriately described by the two-dimensional Mott–Wannier excitons [36]. The nondetection of higher series is an inherent nature of the two-dimensional Mott–Wannier excitons [37], since the intensity of the excitons falls off as $(2n-1)^{-3}$.

As listed in table 1, the transition energies for excitons A and B show a red shift due to the presence of a small amount of Re. The splitting of excitons A and B ($\Delta_{BA} = E_B - E_A$) at 15 K (300 K) are determined to be 415 ± 5 meV (382 ± 13 meV) and 425 ± 5 meV (410 ± 13 meV) for Re-doped and undoped WS_2, respectively. From the recent theoretical and experimental studies [38–41], the A and B excitons are attributed to the smallest direct transitions at the K point of the Brillouin zone split by interlayer interaction and spin–orbit splitting [38–40]. The A exciton belongs to $K_4 \rightarrow K_5$ while the B exciton corresponds to $K_1 \rightarrow K_5$ transitions. The K states have been shown to be predominantly metal d states with a small contribution from the nonmetal p states. The measured difference in the splitting of the A–B excitons for undoped and doped WS_2 shows clear experimental evidence of a distortion of crystal structure which includes modification of the electronic states of the synthesized compounds due to a structural transformation from 2H to 3R polytype. It is very likely that the Re ions can substitute for the W ions and stabilize the 3R polytype of WS_2, which has weaker van der Waals interlayer interaction as reflected by the measured reduction in Δ_{BA}. Our experimental evidence shows the general trend of a reduction of the splitting of excitons A and B for the 3R polytype in agreement with the previous works [14, 42].

Table 1. Transition energy of excitons A and B of WS_2. If a Rydberg series is observed, the energy of the $n = 1$ feature is tabulated. Also included are the corresponding values of previous reports [7, 31–35].

Sample	Temperature (K)	E(A) (eV)	E(B) (eV)	Δ_{BA} E(B) − E(A) (eV)
2H-WS_2[a]				
		2.067 ± 0.002	2.492 ± 0.003	0.425 ± 0.005
	15			
		1.984 ± 0.005	2.394 ± 0.008	0.410 ± 0.013
	300			
3R-WS_2[b]				
		2.039 ± 0.002	2.454 ± 0.003	0.415 ± 0.005
	15			
		1.958 ± 0.005	2.340 ± 0.008	0.382 ± 0.013
	300			
3R-WS_2[c]	5	2.026	2.458	0.422
3R-WS_2[d]	78	2.04	2.45	0.41
3R-WS_2[e]	78	2.06	2.50	0.44
2H-WS_2[f]	300	1.95	2.36	0.41
2H-WS_2[g]	300	1.94	2.36	0.42
2H-WS_2[h]	77	2.06	2.47	0.41
	300	2.0	2.386	0.386

[a] Present work (undoped single crystal, piezoreflectance).
[b] Present work (Re-doped single crystal, piezoreflectance).
[c] Reference [32] (single crystal, transmission).
[d] Reference [33] (single crystal, reflectivity).
[e] Reference [34] (single crystal, reflectivity).
[f] Reference [35] (thin film, transmission).
[g] Reference [36] (thin film, transmission).
[h] Reference [7] (thin film, transmission).

In addition, the effect of the dopant is also clearly manifested in the increase of the broadening parameters Γ_A and Γ_B of the excitonic features A and B. The increase of the broadening parameter for the Re-doped samples is mainly due to impurity scattering.

Displayed by dashed curves in figures 2 and 3 are, respectively, the experimental PzR spectra showing the prominent exciton A and B features for Re-doped and undoped WS_2 at several representative temperatures between 15 and 300 K. The solid curves are the fitted spectral data to equation (1), which yield exciton transition energies indicated by arrows. As a general property of most semiconductors, when the temperature is increased, the exciton A and B transitions in the PzR spectra exhibit energy red-shift and line shape broadening characteristics. The broader line shapes of the excitonic transition features are due to the increase of lattice–phonon scattering effects.

The temperature variations of the energies of A and B excitons for Re-doped and undoped WS_2 are shown in figure 4. Due to the doping effect, bandgap reduction phenomena can also be observed. The solid curves in figure 4 are the least squares fits to the Varshni empirical relationship [28]

$$E_i(T) = E_i(0) - \frac{\alpha_i T^2}{(\beta_i + T)} \tag{3}$$

where $i =$ A or B, $E_i(0)$ is the excitonic transition energy at 0 K and α_i and β_i are constants referred to as the Varshni coefficients. The constant α_i is related to the electron (exciton)–

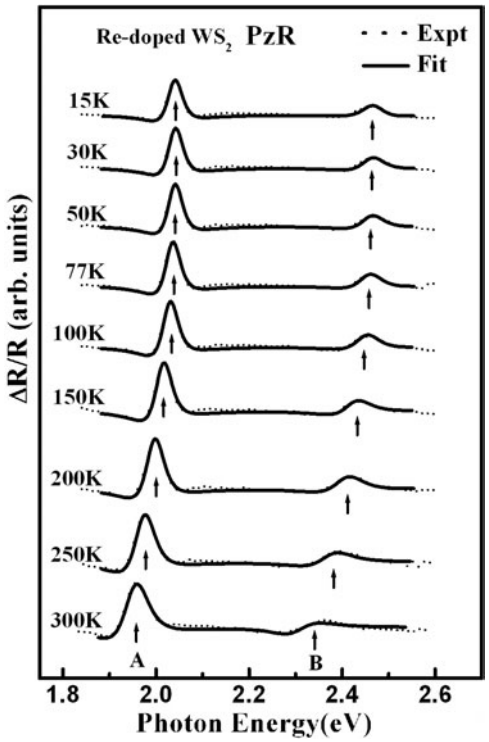

Figure 2. Piezoreflectance spectra of the Re-doped WS_2 at several temperatures between 15 and 300 K. The dashed curves are the experimental curves and the solid curves are least squares fits to equation (1).

phonon interaction and β_i is closely related to the Debye temperature. The obtained values of $E_i(0)$, α_i and β_i for the excitonic transition of Re-doped and undoped WS_2 are listed in table 2. For comparison purposes we have also listed numbers for the A and B excitonic transitions for 2H-$Mo_{1-x}W_xS_2$ [43], 2H-MoS_2 [44] and 3R-MoS_2 [44], and the band-edge excitons of the distorted octahedral layer crystals ReS_2 and $ReSe_2$ [45]. The Debye temperature Θ_D of WS_2 has been estimated to be 210 K using the Lindemann formula by Ho *et al* [43]. The fitted values of β_i are in reasonable agreement with the estimated Θ_D.

The temperature variations of the energies of A_1 and B excitons for Re-doped and undoped WS_2 are also fitted (dashed curves) by an expression containing the Bose–Einstein occupation factor for the phonon in figure 4 [29, 30]:

$$E_i(T) = E_{iB}(0) - a_{iB}\left\{1 + \frac{2}{[\exp(\Theta_{iB}/T) - 1]}\right\} \tag{4}$$

where $i = A_1$ or B, a_{iB} represents the strength of the electron (exciton)–phonon interaction and Θ_{iB} corresponds to the average phonon temperature. The fitted values for $E_{iB}(0)$, a_{iB} and Θ_{iB} are given in table 2, and the corresponding values for 2H-$Mo_{1-x}W_xS_2$ [43], 2H-MoS_2 [44], 3R-MoS_2 [44], ReS_2 and $ReSe_2$ [45] are also listed for comparison.

The experimental values of $\Gamma_i(T)$ (half width at half maximum (HWHM)) of the A_1 and B excitons at several temperatures between 15 and 300 K as obtained from the line shape fit with equation (1) for Re-doped and undoped WS_2 are displayed in figure 5. The temperature

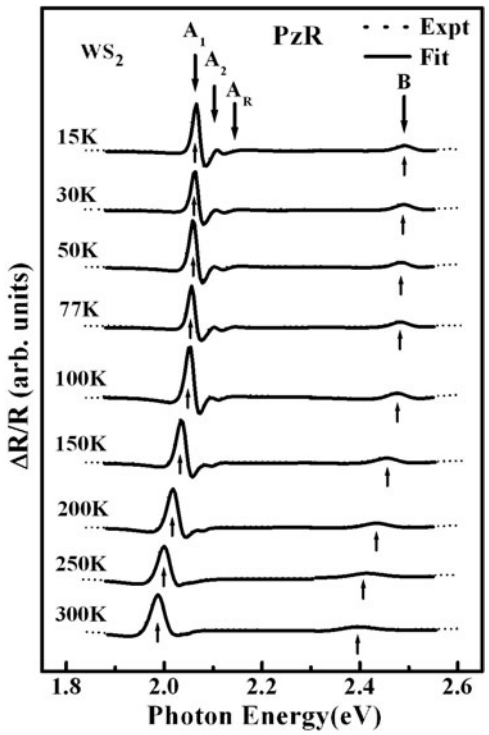

Figure 3. Piezoreflectance spectra of the undoped WS_2 at several temperatures between 15 and 300 K. The dashed curves are the experimental curves and the solid curves are least squares fits to equation (1).

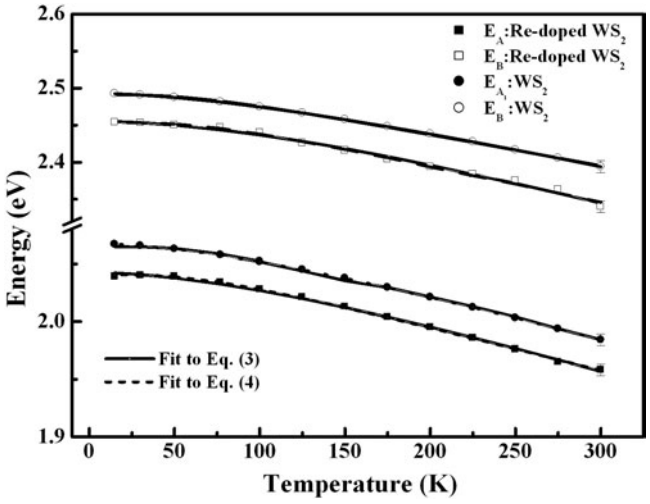

Figure 4. Temperature variations of the A_1 and B excitonic transition energies for Re-doped and undoped WS_2. Representative error bars are shown. The solid curves are least squares fits to equation (3) and the dashed curves are least squares fits to equation (4).

dependence of the broadening parameters of semiconductors can be expressed as [29, 30]

$$\Gamma_i(T) = \Gamma_{i0} + \frac{\Gamma_{i\mathrm{LO}}}{(\exp(\Theta_{i\mathrm{LO}}/T) - 1)} \tag{5}$$

where $i = \mathrm{A}_1$ or B. The first term Γ_{i0} of equation (5) represent the broadening invoked from temperature independent mechanisms, such as electron–electron interaction, impurity, dislocation, electron interaction and alloy scattering, whereas the second term is caused by the electron (exciton)–LO phonon (Fröhlich) interaction. The quantity $\Gamma_{i\mathrm{LO}}$ represents

Table 2. Values of Varshni and Bose–Einstein function fitting parameters describe the temperature dependence of the excitonic transition energies of Re-doped WS_2 and other materials for comparison.

		Varshni			Bose–Einstein		
Material	Feature	$E(0)$ (eV)	α (meV K^{-1})	β (K)	E_{B0} (eV)	a_B (meV)	Θ_B (K)
3R-WS_2[a]	A_1	2.043 ± 0.005	0.49 ± 0.05	215 ± 50	2.041 ± 0.02	38 ± 10	195 ± 40
	B	2.457 ± 0.005	0.64 ± 0.06	215 ± 50	2.455 ± 0.02	46 ± 11	185 ± 35
2H-WS_2[b]	A_1	2.067 ± 0.005	0.47 ± 0.05	210 ± 50	2.105 ± 0.02	41 ± 10	200 ± 40
	B	2.493 ± 0.005	0.55 ± 0.06	200 ± 50	2.530 ± 0.02	40 ± 11	181 ± 35
2H-WS_2[c]	A_1	2.067 ± 0.005	0.47 ± 0.05	210 ± 50	2.102 ± 0.02	37 ± 10	200 ± 40
	B	2.493 ± 0.005	0.55 ± 0.06	200 ± 50	2.534 ± 0.02	45 ± 11	200 ± 35
2H-$Mo_{0.3}W_{0.7}S_2$[c]	A_1	1.979 ± 0.005	0.39 ± 0.05	200 ± 60	2.008 ± 0.02	32 ± 6	200 ± 25
	B	2.338 ± 0.005	0.47 ± 0.06	185 ± 60	2.372 ± 0.02	36 ± 6	185 ± 26
2H-$Mo_{0.5}W_{0.5}S_2$[c]	A_1	1.947 ± 0.005	0.47 ± 0.05	190 ± 60	1.986 ± 0.02	43 ± 12	214 ± 40
	B	2.257 ± 0.005	0.49 ± 0.06	175 ± 60	2.293 ± 0.02	39 ± 10	190 ± 33
2H-$Mo_{0.7}W_{0.3}S_2$[c]	A_1	1.936 ± 0.005	0.46 ± 0.05	190 ± 60	1.977 ± 0.02	43 ± 15	222 ± 50
	B	2.227 ± 0.005	0.38 ± 0.06	175 ± 60	2.255 ± 0.02	30 ± 6	190 ± 25
2H-MoS_2[d]	A_1	1.935 ± 0.005	0.48 ± 0.05	180 ± 50	1.976 ± 0.02	46 ± 15	220 ± 50
	B	2.142 ± 0.005	0.47 ± 0.05	160 ± 50	2.179 ± 0.02	42 ± 8	200 ± 30
3R-MoS_2[e]	A_1	1.918 ± 0.005	0.41 ± 0.05	175 ± 50	1.954 ± 0.01	39 ± 12	215 ± 50
	B	2.072 ± 0.005	0.43 ± 0.05	180 ± 50	2.108 ± 0.01	40 ± 12	210 ± 50
ReS_2[f]	E_1^{ex}	1.554 ± 0.005	0.37 ± 0.05	175 ± 75	1.583 ± 0.008	32 ± 10	200 ± 50
	E_2^{ex}	1.588 ± 0.005	0.39 ± 0.05	170 ± 75	1.619 ± 0.008	34 ± 10	200 ± 50
$ReSe_2$[f]	E_1^{ex}	1.387 ± 0.005	0.45 ± 0.05	175 ± 75	1.428 ± 0.01	45 ± 15	224 ± 75
	E_2^{ex}	1.415 ± 0.005	0.51 ± 0.05	170 ± 75	1.462 ± 0.01	53 ± 20	225 ± 75

[a] Present work (Re-doped single crystal).
[b] Present work (undoped single crystal).
[c] Reference [43].
[d] Reference [44] (undoped single crystal).
[e] Reference [44] (Re-doped single crystal).
[f] Reference [45].

the strength of the electron (exciton)–LO phonon coupling while Θ_{iLO} is the LO phonon temperature [29, 30].

The solid curves in figure 5 are least squares fitted to equation (5), which made it possible to evaluate Γ_{i0}, Γ_{iLO} and Θ_{iLO} for the A and B excitonic transitions of Re-doped and undoped WS_2. The obtained values of these quantities are listed in table 3 together with the numbers for $Mo_{1-x}W_xS_2$ [43], 2H-MoS_2 [44], 3R-MoS_2 [44], ReS_2 [45], $ReSe_2$ [45], GaAs [46] and ZnSe [47].

The parameter α_i of equation (3) is related to a_{iB} and Θ_{iB} of equation (4) by taking the high temperature limit of both expressions and yields $\alpha_i \approx 2a_{iB}/\Theta_{iB}$. Comparison of the numbers listed in table 2 shows that within error bars this relation is satisfied. The temperature shift of excitonic-transition energies is due to both the lattice-constant variations and interactions with relevant acoustic and optical phonons. According to the existing theory [29, 30] this leads to a value of Θ_{iB} significantly smaller than Θ_{iLO}. From tables 2 and 3, it can be seen that our observations are in good agreement with this theoretical consideration.

From table 3, the values of Γ_{i0} for WS_2 are larger than those of most semiconductors. These results agree well with the previous report on MoS_2 by Fortin and Raga [17]. They reported a detailed study on the excitons in MoS_2. The results showed that a very large natural

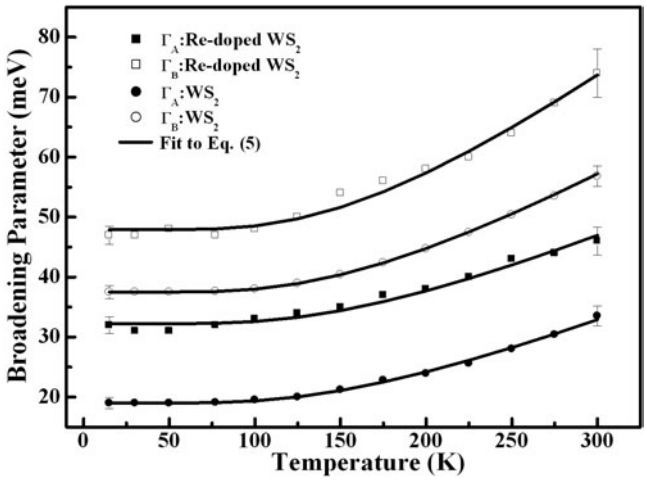

Figure 5. Temperature variations of the broadening parameters of the A_1 and B excitonic transitions for Re-doped and undoped WS_2. Representative error bars are shown. The solid curves are least squares fits to equation (5).

broadening nearly independent of temperature below 100 K characterizes all the excitonic features. A high characteristic temperature was deduced from the half widths of the A_1 and B structures as functions of the temperature and was attributed to a large reduced mass of the excitons. The much larger value of Γ_{i0} for the Re-doped WS_2 is mainly due to impurity scattering. The values of $\Theta_{i\mathrm{LO}}$ are quite close to the previous report of the longitudinal optical phonon temperatures for WS_2 (515 K) obtained from Raman measurements [48]. The close match between the fitted values of $\Theta_{i\mathrm{LO}}$ and the LO phonon temperatures obtained from Raman scattering indicates that the temperature variation of Γ_i is indeed mainly due to the interaction of the electron with optical phonons.

4. Summary

In summary, we have measured the temperature dependence of the energies and broadening parameters of the A and B excitonic transitions of Re-doped and undoped WS_2 single crystals using PzR in the temperature range from 15 to 300 K. The presence of Re has played a major role in influencing the near band-edge excitonic transitions. The electronic states of the Re-doped WS_2 crystals are modified with a red shift of the A and B excitons and a reduction of the energy splitting of A and B excitons. In addition, the effect of the dopant is also clearly manifested in the increase of the broadening parameters Γ_A and Γ_B of the excitonic features A and B. The increase of the broadening parameter for the Re-doped samples is mainly due to impurity scattering. The broader line width and the nature of the two-dimensional Mott–Wannier excitons prevent the detection of higher Rydberg series of the A exciton for the Re-doped sample. The parameters that describe the temperature variations of energies and broadening parameters of the excitonic transitions are evaluated. The temperature shift of excitonic transitions is mainly due to the interaction with relevant acoustic and optical phonons, while the temperature variation of broadening parameter is mainly due to the interaction of the electron (exciton) with optical phonons. The electron (exciton)–phonon coupling constant, Γ_{LO}, for Re-doped and undoped WS_2 are found to be considerably larger than that reported for a number of semiconductors.

Table 3. Values of the parameters which describe the temperature dependence of broadening function $\Gamma(T)$ of the excitonic transitions of Re-doped and undoped WS_2 using equation (5). Relevant values for $Mo_{1-x}W_xS_2$, 2H-MoS_2, 3R-MoS_2, GaAs and ZnSe are included for comparison.

Material	Feature	Γ_0 (meV)	Γ_{LO} (meV)	Θ_{LO} (K)
Re-doped WS_2[a]	A_1	32 ± 1	70 ± 20	525 ± 50
(3R)	B	47 ± 1	115 ± 25	510 ± 50
Undoped-WS_2[b]	A_1	19 ± 1	60 ± 20	520 ± 50
(2H)	B	38 ± 2	90 ± 40	520 ± 50
2H-WS_2[c]	A_1	20 ± 1	50 ± 20	520 ± 50
	B	37.5 ± 2	90 ± 40	520 ± 50
2H-$Mo_{0.3}W_{0.7}S_2$[c]	A_1	41.6 ± 1.0	60 ± 20	530 ± 50
	B	62.2 ± 2.0	75 ± 25	530 ± 50
2H-$Mo_{0.5}W_{0.5}S_2$[c]	A_1	40.5 ± 1.0	85 ± 25	540 ± 50
	B	61.9 ± 2.0	85 ± 30	540 ± 50
2H-$Mo_{0.7}W_{0.3}S_2$[c]	A_1	30.0 ± 1.0	65 ± 20	560 ± 50
	B	62.8 ± 2.0	85 ± 25	560 ± 50
2H-MoS_2[c]	A_1	18.0 ± 1	75 ± 20	560 ± 50
	B	37.4 ± 2	75 ± 35	560 ± 50
Re-doped MoS_2(0.5%)[d]	A_1	15.0 ± 1.0	92 ± 20	510 ± 50
(3R)	B	33.6 ± 1.0	72 ± 20	510 ± 50
Re-doped MoS_2(1%)[d]	A_1	16.4 ± 1.0	85 ± 16	510 ± 50
(3R)	B	34.0 ± 1.0	90 ± 17	520 ± 50
ReS_2[e]	E_1^{ex}	5.5 ± 1.0	74 ± 28	395 ± 100
	E_2^{ex}	7.8 ± 1.0	42 ± 8	363 ± 50
$ReSe_2$[e]	E_1^{ex}	5.7 ± 1.4	67 ± 43	290 ± 100
	E_2^{ex}	8.4 ± 1.5	70 ± 24	385 ± 100
GaAs[f]	E_g	2	20 ± 1	417
ZnSe[g]	E_g	6.5 ± 2.5	24 ± 8	360

[a] Present work.
[b] Present work.
[c] Reference [43].
[d] Reference [44].
[e] Reference [45].
[f] Reference [46].
[g] Reference [47].

Acknowledgment

The authors gratefully acknowledge the support of the National Science Council of Taiwan.

References

[1] Yanagisawa M 1993 *Wear* **168** 167
[2] Fleischauer P D 1987 *Thin Solid Films* **154** 309
[3] Spalvins T 1982 *Thin Solid Films* **96** 17
[4] Martin J M, Donnet C, Le Mogne J and Epicier T 1993 *Phys. Rev.* B **48** 10583
[5] Tributsch H 1977 *Z. Naturf.* a **32** 972
[6] Ouadah A, Pouzet J and Bernède J C 1993 *J. Physique* III **3** 1
[7] Li S J, Bernède J C, Pouzet J and Jamali M 1996 *J. Phys.: Condens. Matter* **8** 2291
[8] Kam K K and Parkinson B A 1982 *J. Phys. Chem.* **86** 463
[9] Jager-Waldau A, Lux-Steiner M, Jager-Waldau R, Burkhardt R and Bucher E 1990 *Thin Solid Films* **189** 339

[10] Baglio J A, Calabrese G S, Kamieniecki E, Kershaw R, Kubiak C P, Ricco A J, Wold A, Wrighton M S and Zoski G D 1982 *J. Electrochem. Soc.* **129** 1461
[11] Baglio J A, Calabrese G S, Harrison D J, Kamieniecki E, Ricco A J, Wrighton M S and Zoski G D 1983 *J. Am. Chem. Soc.* **105** 2246
[12] Santiago-Ortiz Y, Torres G I, Díaz A and Cabrera C R 1995 *J. Electrochem. Soc.* **142** 2770
[13] Tributsch H 1979 *Sol. Energy Mater.* **1** 257
[14] Wilson J A and Yoffe A D 1969 *Adv. Phys.* **18** 193
[15] Mattheiss L F 1973 *Phys. Rev.* B **8** 3719
[16] Khan M R and Goldsmith G J 1983 *Nuovo Cimento* D **2** 665
[17] Fortin E and Raga F 1975 *Phys. Rev.* B **11** 905
[18] Yen P C, Huang Y S and Tiong K K 2004 *J. Phys.: Condens. Matter* **16** 2171
[19] Hu S Y and Tiong K K 2004 unpublished
[20] Agarwal M K, Patel P D and Gupta S K 1993 *J. Cryst. Growth* **129** 559
[21] Legma J B, Vacquier G, Traorè H and Casalot A 1991 *Mater. Sci. Eng.* B **8** 167
[22] Lévy F, Schmid P and Berger H 1976 *Phil. Mag.* **24** 1129
[23] Zelikman A N, Indenbaum G V, Teslitskaya M V and Shalankova V P 1970 *Sov. Phys.—Crystallogr.* **14** 687
[24] Clark A H 1970 *N. Jahrbuch Mineral. Monatshefte* **3** 33
[25] Pollak F H and Shen H 1993 *Mater. Sci. Eng.* R **10** 275
[26] Mathieu H, Allègre J and Gil B 1991 *Phys. Rev.* B **43** 2218
[27] Aspnes D E 1980 *Optical Properties of Semiconductors* (*Handbook on Semiconductors* vol 2) ed M Balkanski (Amsterdam: North-Holland) p 109
[28] Varshni Y P 1967 *Physica* **34** 149
[29] Lantenschlager P, Garriga M, Logothetidis S and Cardona M 1987 *Phys. Rev.* B **35** 9174
[30] Lantenschlager P, Garriga M, Viña L and Cardona M 1987 *Phys. Rev.* B **36** 4821
[31] Wildervanck J C and Jellinek F 1971 *J. Less-Common Met.* **24** 73
[32] Beal A R, Knights J C and Liang W Y 1972 *J. Phys. C: Solid State Phys.* **5** 3540
[33] Liang W Y 1973 *J. Phys. C: Solid State Phys.* **6** 551
[34] Beal A R, Liang W Y and Hughes H P 1976 *J. Phys. C: Solid State Phys.* **9** 2449
[35] Ballif C, Regula M, Schmid P E, Remškar M, Sanjinés R and Lévy F 1996 *Appl. Phys.* A **62** 543
[36] Tonti D, Varsano F, Decker F, Ballif C, Regula M and Remškar M 1997 *J. Phys. Chem.* B **101** 2485
[37] Beal A R and Liang W Y 1976 *J. Phys. C: Solid State Phys.* **9** 2459
[38] Klein A, Tiefenbacher S, Eyert V, Pettenkofer C and Jaegermann W 2001 *Phys. Rev.* B **64** 205416
[39] Coehoorn R, Hass C, Dijkstra J, Flipse C J F, de Groot R A and Wold A 1987 *Phys. Rev.* B **35** 6195
[40] Coehoorn R, Hass C and de Groot R A 1987 *Phys. Rev.* B **35** 6203
[41] Sourisseau C, Fouassier M, Alba M, Ghorayeb A and Gorochov O 1989 *Mater. Sci. Eng.* B **3** 119
[42] Clark A and Williams R H 1968 *J. Phys. D: Appl. Phys.* D **1** 1222
[43] Ho C H, Wu C S, Huang Y S, Liao P C and Tiong K K 1998 *J. Phys.: Condens. Matter* **10** 9317
[44] Tiong K K, Shou T S and Ho C H 2000 *J. Phys.: Condens. Matter* **12** 3441
[45] Ho C H, Huang Y S, Liao P C and Tiong K K 1998 *Phys. Rev.* B **58** 12575
[46] Qiang H, Pollak F H, Sotomayor Torres C M, Leitch W, Kean A H, Stroscio M, Iafrate G J and Kim K W 1992 *Appl. Phys. Lett.* **61** 1411
[47] Malikova L, Krystek W, Pollak F H, Dai N, Cavus A and Tamargo M C 1996 *Phys. Rev.* B **54** 1819
[48] Ushida S I and Tanaka S 1978 *J. Phys. Soc. Japan* **45** 153